# ON THE ANISOTROPY OF THE LINEAR MECHANISM OF AERODYNAMIC SOUND GENERATION BY VORTICAL PERTURBATIONS IN SHEAR FLOWS

**Jan-Niklas Hau**
Chair of Fluid Dynamics
TU Darmstadt
Otto-Berndt-Str. 2, 64287 Darmstadt, Germany
hau@fdy.tu-darmstadt.de

**Martin Oberlack**
Chair of Fluid Dynamics
TU Darmstadt
Otto-Berndt-Str. 2, 64287 Darmstadt, Germany

**George Chagelishvili**
Abastumani Astrophysical Observatory
Ilia State University
Tbilisi 0160, Georgia

## ABSTRACT

We investigate the basics of the linear generation of acoustic waves by vortex modes in homentropic compressible flows with constant shear of velocity, $\mathbf{U}_0 = (Ay, 0, 0)$. The mathematical and physical aspects of the generation are grasped by analyzing the dynamics of single, up-shear tilted pure vortex spatial Fourier harmonics (SFHs). The key to comprehending the wave generation process is the possibility of splitting the perturbation field of the considered SFH into its vortex and wave parts at the moment of abrupt wave emergence. Essentially, the linear wave generation mechanism by vortex SFHs in three dimensions (3-D) is similar as in two dimensions (2-D), whereas latter dominates the generation process. The anisotropy of this linear mechanism is also active in 3-D and, thus, confirms the conclusion drawn by Hau *et al.* (2015) that the anisotropic linear generation mechanism is missed by any formulation of an acoustic analogy as introduced by Lighthill (1952, 1954) due to their topological incompatibility.

## 1 INTRODUCTION

The generation of acoustic waves by (turbulent/coherent) vortices is a central problem when it comes e.g., to the design of turbomachinery and jet engines. The principal differences between linear and nonlinear mechanisms of acoustic wave generation by vortex perturbations in shear flows is found in the strength, geometry of propagation and length/time scales of the generated waves. In the 1990s there has been a breakthrough in the understanding of non-uniform/shear flow dynamics. Their mathematical specificity was revealed and proven (see e.g., Schmid & Henningson (2001) and references herein), i.e., when applying modal analysis, the appearing operators are non-normal and, consequently, the corresponding eigenmodes are non-orthogonal. Due to this, the eigenmodes interfere and *ergo* a suitable approach needs to be applied to analyze this. Discarding the modal analysis and adopting the so-called nonmodal approach these issues are circumvented and the transient dynamics can be grasped. Originally devised by Lord Kelvin (1887), one formulation of the nonmodal approach consists of the transformation from the laboratory frame of reference to one co-moving with the flow and then studying the evolution of SFHs without spectral expansion in time. This is one of a family of Ansatz functions for flows with constant shear of velocity (Hau *et al.*, 2017). Yoshida (2005) has been mathematically proven that the Kelvin mode approach represents the optimal technique for stability studies of constant shear flows.

## 2 BASIC GOVERNING EQUATIONS

We linearize the compressible Euler equations about a 3-D homentropic (uniform pressure/density) flow with constant velocity shear $\mathbf{U}_0 = (Ay, 0, 0)$, $A > 0$, assuming that the disturbances are adiabatically compressible with constant speed of sound $c_s$, $p = c_s^2 \rho$:

$$\begin{gathered}\left[\frac{\partial}{\partial t} + Ay\frac{\partial}{\partial x}\right]\frac{\rho}{\rho_0} + \left(\frac{\partial}{\partial x}u_x + \frac{\partial}{\partial y}u_y + \frac{\partial}{\partial z}u_z\right) = 0\,, \\ \left[\frac{\partial}{\partial t} + Ay\frac{\partial}{\partial x}\right]u_x + Au_y + c_s^2\frac{\partial}{\partial x}\frac{\rho}{\rho_0} = 0\,, \\ \left[\frac{\partial}{\partial t} + Ay\frac{\partial}{\partial x}\right]u_y + c_s^2\frac{\partial}{\partial y}\frac{\rho}{\rho_0} = 0\,, \\ \left[\frac{\partial}{\partial t} + Ay\frac{\partial}{\partial x}\right]u_z + c_s^2\frac{\partial}{\partial z}\frac{\rho}{\rho_0} = 0\,.\end{gathered} \tag{1}$$

Employing the Kelvin mode approach, SFHs of perturbations with time-dependent shearwise wavenumber $k_y(t) = k_y(0) - Ak_x t$ are introduced: $\psi(\mathbf{x},t) = \tilde{\psi}(t)\exp(\mathrm{i}\mathbf{k}(t)\cdot\mathbf{x})$, where $\psi = (u_x, u_y, u_z, \rho)$, $\mathbf{x} = (x, y, z)$, $\mathbf{k} = (k_x, k_y, k_z)$. This reduces the system of PDEs to one of ODEs. Moreover, the

following non-dimensional variables are introduced:

$$\begin{gathered}\kappa(\tau)=|\mathbf{k}(t)|/k_x=\sqrt{1+\beta^2(\tau)+\gamma^2}\ ,\\ \beta(\tau)=k_y(0)/k_x-\mathscr{M}\tau=\beta(0)-\mathscr{M}\tau\ ,\\ \hat{\mathbf{x}}=k_x\mathbf{x}\ ,\ \tau=c_sk_xt\ ,\mathscr{M}=A/(k_xc_s)\ ,\ \gamma=k_z/k_x\ ,\\ D=\mathrm{i}\tilde{\rho}/\rho_0\ ,\ \mathbf{v}=\tilde{\mathbf{u}}/c_s\ ,\mathbf{V}_0=\mathbf{U}_0/c_s\ .\end{gathered}\tag{2}$$

Hence, the set of ODEs in time is given by:

$$\begin{aligned}&\frac{\mathrm{d}}{\mathrm{d}\tau}v_x=-\mathscr{M}v_y-D\ ,\quad \frac{\mathrm{d}}{\mathrm{d}\tau}v_y=-\beta(\tau)D\ ,\\ &\frac{\mathrm{d}}{\mathrm{d}\tau}v_z=-\gamma D\ ,\quad \frac{\mathrm{d}}{\mathrm{d}\tau}D=v_x+\beta(\tau)v_y+\gamma v_z\ .\end{aligned}\tag{3}$$

Eqs.(3) allow the formulation of an invariant in time

$$\mathscr{W}=(1+\gamma^2)v_y-\beta(\tau)(v_x+\gamma v_z)-\mathscr{M}D\ ,\ \frac{\mathrm{d}\mathscr{W}}{\mathrm{d}\tau}=0\ ,\tag{4}$$

which corresponds to the conservation of the potential vorticity (PV) in $\mathbf{k}$-space and is important in the analysis of wave–vortex systems in smooth shear flows, indicating the existence of vortex perturbations (Hau *et al.*, 2015). As suggested by Chagelishvili *et al.* (1997*a*), we introduce an auxiliary variable $\xi=v_x+\gamma v_z$. By doing so, the system of ODEs reduces by one equation, which can be reformulated only in $\xi$ using Eq.(4)

$$\frac{\mathrm{d}^2}{\mathrm{d}\tau^2}\xi+\omega^2(\tau)\xi=-\beta(\tau)\mathscr{W}\ ,\tag{5}$$

with $\omega(\tau)=\sqrt{1+\beta^2(\tau)+\gamma^2}$. Eq.(5) has the form of a wave-equation with a source term on the right hand side, proportional to $\mathscr{W}$. It describes two types of disturbances: (i) Acoustic wave SFHs, $\xi^{(\mathrm{w})}$, ($\mathscr{W}=0$ and non-zero group velocity) which are described by the general solution of the corresponding homogeneous equation; (ii) Vortex SFHs, $\xi^{(\mathrm{v})}$, ($\mathscr{W}\neq 0$ and zero group velocity) that originate from the inhomogeneity, $\beta(\tau)\mathscr{W}$, and are associated with the particular solution. The vortex mode amplitude is proportional to $\mathscr{W}$, i.e., is zero when $\mathscr{W}=0$. The character of the shear flow dynamics depends on the initially imposed *pure* vortex or wave mode disturbance. While latter is to realize straightforward ($\mathscr{W}=0$) and has been analyzed by Chagelishvili *et al.* (1997*a*), the extraction of pure vortex modes is not, as the Kovasznay decomposition does not hold (Goldstein, 2013). At the same time, the separation of the described disturbance modes by the value of the PV is efficient and has been widely used by the atmospheric community (see e.g., McIntyre (2009) and references herein) to study the generation of inertia–gravity waves (having zero PV) by PV disturbances. Although the aperiodic vortex mode is uniquely determined, the correspondence between a vortex mode and a particular solution of the inhomogeneous equation is not unique. The evolution of $v_x$ and $v_z$ depends on the wavenumber ratio $\gamma$, yet, the evolution of $\xi$ is identical to the one of $v_x$ in the 2-D case, but with $\gamma$-dependent frequency $\omega(\tau)$.

We introduce the dynamical Mach number as $\mathscr{M}_D(\tau)\equiv A/(c_sk(t))=\mathscr{M}/(\kappa(\tau))$, which is a measure for the compressibility of any SFH in time. The maximum of $\mathscr{M}_D$, i.e., maximum compressibility characteristic, is reached when the SFH crosses the $k_x$-axis (line of $k_y=0$) at $\tau^*=\beta(0)/\mathscr{M}^*$:

$$\mathscr{M}^*\equiv\max(\mathscr{M}_D(\tau))=\frac{\mathscr{M}}{\sqrt{1+\gamma^2}}\ .\tag{6}$$

$\mathscr{M}^*$ defines the strength of the linear mode-coupling. For $\mathscr{M}_D\ll 1$ it becomes possible to determine vortex mode harmonics in regions where $\beta(0)\gg 1$ in the manner suggested by Hau *et al.* (2015). Here, the compressibility characteristic of the vortex mode harmonic substantially diminishes and the separation between vortex and acoustic wave modes becomes possible. This enables us to study the generation of wave mode perturbations by initially pure (void of acoustic wave) vortex modes.

We seek the smoothly monotonic vortex mode solution in the spectral plane in some point $(k_x,k_y(0))$ with $\beta(0)\gg 1$ in the following asymptotic analytic form:

$$\xi(0)\equiv\xi^{(0)}(0)+\xi^{(1)}(0)+\ldots+\xi^{(n)}(0)+\ldots\ .\tag{7}$$

The zero-approximation term of Eq.(5) for large $\beta(0)$ leads to the neglect of the term including the second derivative and, thus, gives

$$\xi^{(0)}(\tau)=\frac{\beta(\tau)}{\omega^2(\tau)}\mathscr{W}(\beta(0),\gamma)\ .\tag{8}$$

In the nonmodal approach this condition usually defines the vortex mode. However, the impurity by waves, i.e., any oscillating behavior, can be minimized by taking into account the corrections of the second derivative. The first correction gives

$$\xi^{(1)}(0)=-\left[\frac{1}{\omega^2(\tau)}\frac{\mathrm{d}^2\xi^{(0)}(\tau)}{\mathrm{d}\tau^2}\right]_{\tau=0}\ ,\tag{9}$$

which then generally leads to the following iterative steps:

$$\xi^{(n)}(0)=-\left[\frac{1}{\omega^2(\tau)}\frac{\mathrm{d}^2\xi^{(n-1)}(\tau)}{\mathrm{d}\tau^2}\right]_{\tau=0}\ .$$

In fact, the first two terms of this series are a good approximation to the exact numerical solution inside the adiabatic region. Hence, we calculate $\xi(0)$ for the vortex mode disturbances by inserting Eqs.(8)-(9) into (7). From this also the first derivative can be calculated, which is necessary to recover $v_y$ and $D$.

In contrast to the oscillating and propagating wave mode perturbations, vortex mode perturbations relate to the smoothly monotonic, non-oscillating and, consequently, non-propagating aperiodic part of the solution in any region of the wavenumber space.

Finally, the auxiliary dependent variable $\xi(\tau)$ needs to be split into the streamwise and spanwise velocity perturbations in the adiabatic limit (Chagelishvili *et al.*, 1997*a*), i.e., $\mathscr{M}_D\ll 1$:

$$v_x(0)=\xi(0)\frac{1}{1+\gamma^2}-\gamma C\ ,\quad v_z(0)=\xi(0)\frac{\gamma}{1+\gamma^2}+C\ .\tag{10}$$

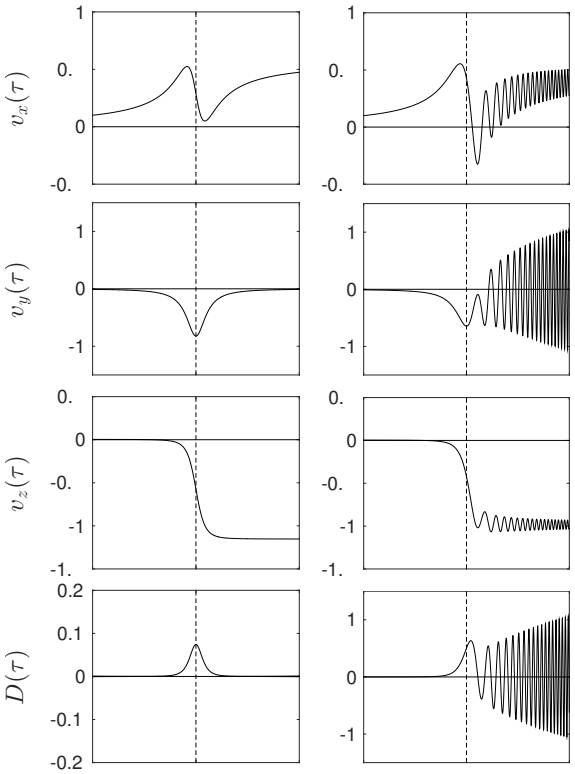


Figure 1: Dynamics of $v_x, v_y, v_z, D$ for $\mathscr{M}^* = [0.05, 0.4]$ from left to right for $\gamma = 0.5$, $C = 0$.

Here, $v_x$ and $v_z$ are defined up to a constant $C$, which meaning is known from the solutions of the incompressible dynamics (Moffatt, 1967) and needs to be considered in the analysis of the compressible case. In fact, the constant accounts for the fact that the stream- and spanwise velocity perturbations only occur independently from each other in the derivatives of the considered system (3)-(4). Apart from the derivatives, $v_x$ and $v_z$ only occur in the combination $\xi = v_x + \gamma v_z$. Therefore, the pure vortex solution initially only fixes $\xi(0)$ and, so, the values of $v_x(0)$ and $v_z(0)$ can be arbitrary if (i) their combination gives the required value of $\xi(0)$ *and* (ii) derivatives of $\mathrm{d}v_x/\mathrm{d}\tau$ and $\mathrm{d}v_z/\mathrm{d}\tau$ in Eq.(3) vary slowly and monotonically at $\beta(0) \gg 1$ ($\mathscr{M}_D \ll 1$). The remaining quantities can be calculated in terms of $\xi$. The results obtained by solving the system of ODEs (3) for vortex mode harmonics as initial conditions with different values of $\mathscr{M}^*$, $\gamma$ and $C$ is presented in the following section.

## 3 RESULTS

In comparison with its 2-D counterpart, the 3-D dynamics are more complex regarding the degrees of freedom in the free non-dimensional parameters. Specifically, in 2-D we only have to take into account the wavenumber-ratio $\beta(0)$ and $\mathscr{M} = A/(k_x c_s)$. This set of parameters is enlarged by $\gamma$ and the free parameter $C$, while the perturbation Mach number changes to $\mathscr{M}^* = \mathscr{M}/\sqrt{1+\gamma^2}$.

In Fig.1 we present the dynamics of a single Kelvin mode at different perturbation Mach numbers $\mathscr{M}^* = [0.05, 0.2, 0.4]$ with $\gamma = 0.5$, $\beta(0) = 10$ and $C = 0$. The absence of any oscillating part in the solution for $\tau < \tau^*$ confirms the correct extraction of the aperiodic part as initial conditions. The dynamics are comparable to the 2-D counterpart and the critical time $\tau^* = \beta(0)/\mathscr{M}^*$ is a universal

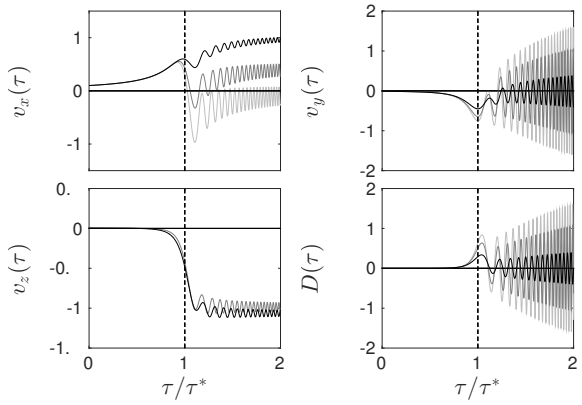


Figure 2: Dynamics of $(v_x, v_y, v_z, D)$ for $\mathscr{M}^* = 0.4$, $\beta(0) = 10$, $C = 0$ and $\gamma = [0, 0.5, 1]$ (from light to dark).

timescale for the appearance of linearly generated waves. This phenomenon becomes visible by naked-eye for moderate values of the perturbation Mach number by the appearance of high frequency oscillations, as in the 2-D case (Chagelishvili *et al.*, 1997*b*). The most eye-catching difference in the dynamics, compared to the limiting 2-D case, lies in the fact that (i) the dynamics of the streamwise velocity perturbations are no longer (point) symmetric about the critical time, (ii) the appearance of an additional perturbation velocity ($v_z$), and (iii) the ongoing amplification of vortex as well as wave harmonics for $\tau > \tau^*$ (see also (Moffatt, 1967; Chagelishvili *et al.*, 2016)). The dynamics of the shearwise velocity and density perturbations are rather unaffected by the additional space-dimension.

We present the analysis of the dynamics of initially pure vortex SFHs depending on $\gamma = k_z/k_x$ in Fig.2 for the primitive variables, where $\mathscr{M}^* = 0.4, \beta(0) = 10, C = 0$ and $\gamma = [0, 0.5, 1]$. The dynamics of the respective perturbation quantities are presented superimposed onto each other. Here the gray-scale varies from light to dark with increasing value of $\gamma$. Firstly, the most striking difference in the dynamics is found in the amplitude of the oscillations that appear after the critical time, which indicates a reducing influence of the 3-D dynamics in contrast to 2-D. Secondly, one recognizes the influence on the streamwise and spanwise perturbation velocities. Of course the latter is absent for $\gamma = 0$, the 2-D case.

As aforementioned, the exact solution of the incompressible counterpart is well known and exhibits the free parameter $C$ (Moffatt, 1967), which allows some freedom in the solution and has an impact on the energy growth of the regarded Kelvin mode. To evaluate this, we solve the system of ODEs (3) for a fixed $\gamma$ and different values of $C$, resulting in a change of the initial conditions of the streamwise and shearwise velocity perturbations, $v_x(0)$ and $v_z(0)$, respectively:

$$v_x'(0) = v_x(0) - \gamma C\,, \quad v_z'(0) = v_z(0) + C\,, \tag{11}$$

where the primed values are the new initial conditions, depending on the choice of $C$. This change is best observed in Fig.3. Here, the dynamics in the dependent variables is presented for $\gamma = 1$, $\mathscr{M}^* = 0.4$ and three different values of $C = [-0.5, 0, 0.5]$. The dynamics in the shearwise velocity and density perturbations remain unchanged throughout the

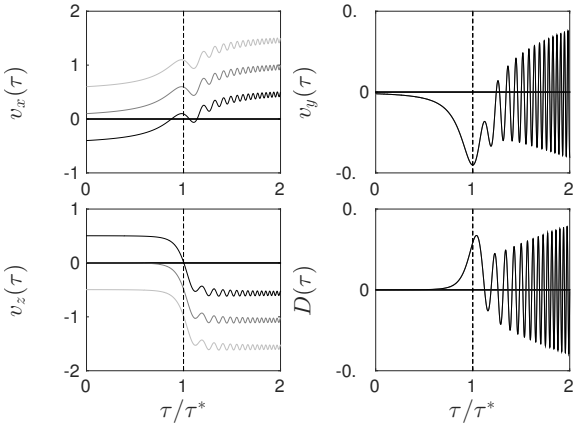


Figure 3: Dynamics of $(v_x, v_y, v_z, D)$ for $\mathscr{M}^* = 0.4$, $\beta(0) = 10$, $\gamma = 1$ and $C = [-0.5, 0, 0.5]$ (from light to dark).

choice of $C$, whereas the values and thus, the further evolution of the streamwise and spanwise velocity perturbations is shifted. In fact, a variation of $C$, although changing $v_x(0)$ and $v_z(0)$, does not affect the wave generation process.

We follow a similar path as taken in Refs. (Chagelishvili *et al.*, 1997*b*; Hau *et al.*, 2015) in order to uncouple the dynamics of vortex and wave mode perturbations. This analysis is of purely numerical nature (strictly speaking non-physical but mathematical) and allows to understand the different behaviors of vortex and wave modes in the further dynamics. Although they are not distinguishable inside the energy gaining region ($|\beta| < 1$), the mathematical separation is insightful. In Fig.4 we present the results of the split quantities for $\mathscr{M}^* = 0.4, \beta(0) = 10, \gamma = 1, C = 0$.

We summarize the main results of the splitting in the following: (i) There is an abrupt emergence of waves from vortices; (ii) The jumps that occurs in the evolution $v_x^{(\mathrm{v})}$ and $v_z^{(\mathrm{v})}$ characterize the spontaneously generated wave mode. (iii) The vortex and wave parts of the quantities evolve independently from each other – vortex SFHs approach a fixed state, whereas wave SFHs grow linearly in time for $\tau > \tau^*$ with the growth of $|\omega(\tau)|$, i.e., wave and vortex parts are just superimposed onto each other; (iv) The PV $\mathscr{W}$ (see Eq.4) equals to zero for the wave (w) parts, whereas it is conserved for the vortex (v) parts. Moreover, the proposed splitting allows to quantify the efficacy of the wave generation process by initially pure vortex SFHs. This is identified by the jump occurring in the vortex part of the split dependent variables at $\tau = \tau^*$ and the thereby generated wave SFH. The jump naturally occurs in the derivatives of the remaining quantities. Thus, we define the efficacy $\eta$ (can be larger than one) as the ratio of vortex to wave energy:

$$\eta \equiv \frac{E_{\mathbf{k}}^{(\mathrm{w})}(\tau_+^*)}{E_{\mathbf{k}}^{(\mathrm{v})}(\tau_-^*)} = \frac{|\mathbf{v}^{(\mathrm{w})^2}(\tau_+^*)| + |D^{(\mathrm{w})^2}(\tau_+^*)|}{|\mathbf{v}^{(\mathrm{v})^2}(\tau_-^*)| + |D^{(\mathrm{v})^2}(\tau_-^*)|}\,, \qquad (12)$$

with $\tau = \tau^* \pm 0 \equiv \tau_\pm^*$. In Fig.5(a) the efficacy of the wave generation phenomenon in a plane 3-D shear flow is illustrated. In the 3-D case the effective Mach number is reduced by the factor $\sqrt{1+\gamma^2}$, which reduces the efficiency of the wave generation, thus, 2-D SFHs are more efficient. In Fig.5(b) the dependence of $\eta$ on $C$ is presented. The linear mechanism of wave generation by vortex SFHs is strongest for 2-D perturbations for $C = 0$. While, for 3-D harmonics ($\gamma \neq 0$) the strongest emergence of linearly generated waves is shifted away from $C = 0$ depending on $\gamma$. The direction of the shifting is defined by the sign of $\gamma$.

Due the peculiarity of the wave generation process – this takes place just at times when vortex SFHs cross the axis of $k_y = 0$ – initially, all generated wave SFHs have zero shearwise wavenumbers. This leads to a specific, regular wave front and trajectory of the linearly generated waves. We estimate this trajectory in the WKB approximation. Although the rays quantitatively somehow differ from the initial stage of the generated wave propagation for moderate Mach numbers, it has been shown that they reliably predict the linear wave propagation phenomenon in a 2-D shear flow (Hau *et al.*, 2015).

We define the total wave velocity $\mathbf{V}^T$ by the sum of the wave's group and base flow velocity

$$\mathbf{V}^T = \mathbf{V}^G + \mathbf{V}_0 = \mathbf{V}^G + (\mathscr{M}\hat{y}, 0, 0)\,. \qquad (13)$$

The coordinates of the emitted wave-fronts are given by

$$\begin{aligned} \hat{x}(\tau) &= \int_{\tau^*}^{\tau} \mathrm{d}\tau' [V_{\hat{x}}^G(\tau') + \mathscr{M}\hat{y}(\tau')]\,, \\ \hat{y}(\tau) = \int_{\tau^*}^{\tau} \mathrm{d}\tau' V_{\hat{y}}^G \quad &\text{and} \quad \hat{z}(\tau) = \int_{\tau^*}^{\tau} \mathrm{d}\tau' V_{\hat{z}}^G\,. \end{aligned} \qquad (14)$$

The time-dependent wave group velocity $\mathbf{V}^G$ can be calculated via the definition for the instant frequency $\omega = \pm\sqrt{1+\beta^2(\tau)+\gamma^2}$, representing the spectral characteristics of acoustic wave SFHs. So, we write for the non-dimensional group velocity $\mathbf{V}^G$:

$$\mathbf{V}^G = \left( \pm\frac{1}{\omega(\tau)}\,,\ \pm\frac{\beta(\tau)}{\omega(\tau)}\,,\ \pm\frac{\gamma}{\omega(\tau)} \right)\,. \qquad (15)$$

At $\tau = \tau^*$, $\beta(\tau^*) = 0$ and the group velocity is directed inside the $(x,z)$-plane and two rays are emitted in opposite directions inside this plane. These properties only gain importance for wave packets, when the ray theory (i.e., the WKB approximation) makes sense. Accordingly the rays can be calculated from relation (15). We omit the presentation of the full equations here for the sake of brevity. Rather, the ray trajectories are illustrated in Fig.6 for $\mathscr{M} = 0.1$, $\gamma = 0.5$ and $\beta(\tau^*) = 0$, emerging from one single point, for the sake of simplicity, neglecting the size of the emitting area. The trajectories are determined by the signs of the shear parameter and the wavenumbers. In our case the shear parameter is assumed to be positive, $\mathscr{M} > 0$, thus, $\beta(\tau) < 0$ at $\tau > \tau^*$ and asymptotically the inclination is zero:

$$\lim_{\tau\to\infty} \frac{\mathrm{d}\hat{y}}{\mathrm{d}\hat{x}} = \lim_{\tau\to\infty} \frac{\mathrm{d}\hat{y}(\tau)/\mathrm{d}\tau}{\mathrm{d}\hat{x}(\tau)/\mathrm{d}\tau} = 0\,. \qquad (16)$$

The two rays turn in $y$-direction, as $\beta(\tau) < 0$ (correspondingly $V_y^G(\tau) \neq 0$) and are additionally carried backwards by the mean flow, propagating antisymmetrically in time (Eq.(15)). As $\beta(\tau^*) = 0$ for all linearly generated waves, $\mathbf{V}^G$ is directed inside the $(x,z)$-plane at the moment of generation and two rays are emitted in opposite directions inside this plane. This peculiarity is inherent for linearly generated waves, whereas there is a broad spectrum of nonlinearly generated wave harmonics in $k_y$ for each $k_x$. It follows

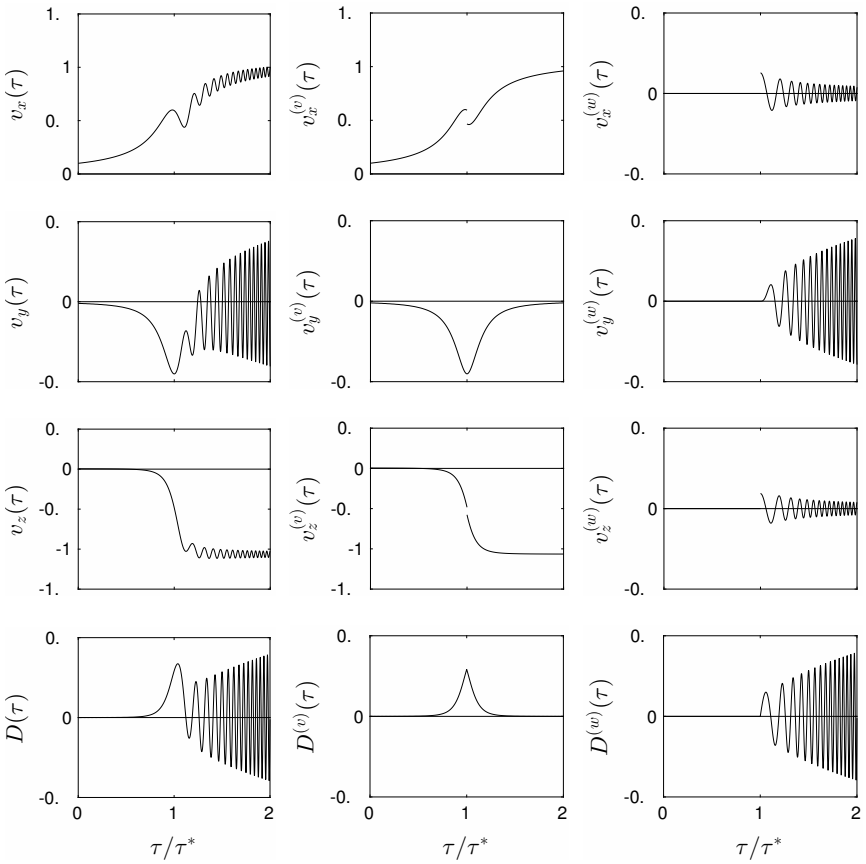


Figure 4: Dynamics of $(v_x, v_y, v_z, D)$, their vortex (v) and wave parts (w) for an initially pure vortex disturbance $(v_x^{(\mathrm{w})}(0), v_y^{(\mathrm{w})}(0), v_z^{(\mathrm{w})}(0), D^{(\mathrm{w})}(0) = 0)$ for $\mathscr{M}^* = 0.4, \beta(0) = 10, \gamma = 1, C = 0$. An abrupt emergence of waves from the initial vortex mode at $\tau = \tau^*$ is observed. The amplitude of the generated wave $v_x^{(\mathrm{w})}(\tau^*)$ smooths the jump appearing in the aperiodic mode of $v_x, v_z$.

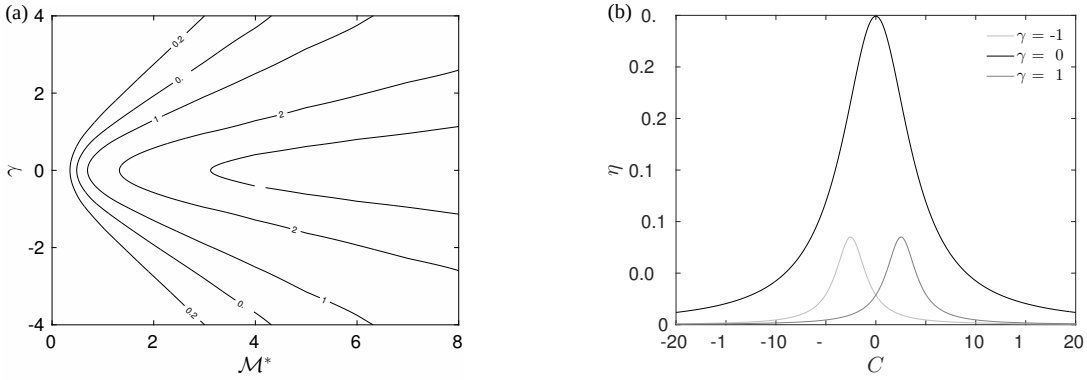


Figure 5: Efficacy of the linear wave generation $\eta$ depending on (a) the perturbation Mach number $\mathscr{M}$ and wavenumber ratio $\gamma = k_z/k_x$, $C = 0$ and (b) on the free parameter $C$, where $\mathscr{M}^* = 0.4$, while $\gamma = [-1, 0, 1]$. The wavenumber ratio $\beta = k_y(0)/k_x$ is always $\beta = 10$.

that each ray trajectory of nonlinearly generated waves is different, due to the broad spectrum of wavenumbers in $k_y$ and it is impossible to obtain a comparable wavenumber-relation as in the linear case. The difference between linear and nonlinearly generated waves manifests itself in an irregular front and an almost omni-directivity (however, weakened by the shear) of nonlinearly generated sound, thus, providing a well distinguishable counterpart to the linear one. These observations match with the ones for a developing shear layer (Avital *et al.*, 1998) and the two-noise source model in jets (Tam, 1995).

Although not presented in this place, we stress that the mechanical picture of the transient growth of vortex mode harmonics that has recently been constructed by Chagelishvili *et al.* (2016) by analyzing the dynamics of a single vortex SFH (with $k_y(0)/k_x > 0$) in an unbounded, incompressible and inviscid base flow with constant shear of velocity $\mathbf{U} = (Ay, 0, 0)$, can naturally be extended to the

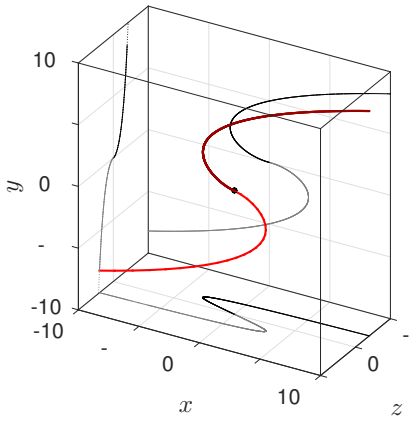


Figure 6: Illustration of the trajectories of a linearly generated wave (red and dark red) together with their projections on the different planes (black and gray). At the moment of its generation $\beta(\tau^*) = 0$. The following parameters are chosen for the visualization: $\mathscr{M} = 0.1$, $\gamma = 0.5$.

compressible dynamics. Here, the widely accepted way of investigating fluid or plasma instabilities was applied, namely, introducing (virtual) fluid particles that undergo a small spatial shift in the flow and subsequently analyzing the resulting variance of the forces acting on those. It was shown that the dynamically generated pressure perturbation field governs the process of transient growth. This dynamics involves (i) the formation of the pressure perturbation field in the shear flow that can be understood as the result of counter-moving neighboring sets of fluid particles in the flow; (ii) the feedback of the pressure field on the dynamics of fluid particles. By analyzing the compression of the medium (i.e., a continuous rise of the pressure perturbations) due to counter-moving neighboring sets of fluid particles in the flow and analyzing the feedback of the generated pressure field on the movement of the fluid particles, the finite value of the sound speed in the compressible case is taken into account. This causes a delay of the adjustment of the fluid particles velocity to the pressure field. Hence, the velocity perturbation does not instantaneously follow the turning of the maximum pressure line, always lagging behind. This lag is crucial in the process of wave generation and manifests itself in a decompression process for $t > t^*$.

The presented investigation reveals that the linear mechanism of the acoustic wave generation by vortex mode perturbations in 3-D follows similar dynamics as in the 2-D, despite the free parameter $C$. At the critical time $t = t^* \equiv k_y(0)/k_x$, the vortex part *fully adopts the potential vorticity* and in the down-shear tilted phase, $k_y(t)/k_x < 0$, evolves aperiodically. At the same time, the wave part *has zero potential vorticity* and further exhibits an oscillating nature, being also down-shear tilted. However, in the 3-D case the effective Mach number is reduced by the factor $\sqrt{1+\gamma^2}$. This reduces the efficiency of wave generation, which maximum depends on the value of $C$, and stresses the predominance of 2-D harmonics in the process of linear acoustic wave generation.

## REFERENCES


Avital, E. J., Sandham, N. D. & Luo, K. H. 1998 Mach wave radiation by mixing layers. Part I: Analysis of the sound field. *Theor. Comput. Fluid Dyn.* **12**, 73–90.

Chagelishvili, G., Hau, J.-N., Khujadze, G. & Oberlack, M. 2016 Mechanical picture of the linear transient growth of vortical perturbations in incompressible smooth shear flows. *Phys. Rev. Fluids* **1** (4), 043603.

Chagelishvili, G., Khujadze, G., Lominadze, J. & Rogava, A. 1997*a* Acoustic waves in unbounded shear flows. *Phys. Fluids* **9**, 1955–1962.

Chagelishvili, G., Tevzadze, A., Bodo, G. & Moiseev, S. 1997*b* Linear mechanism of wave emergence from vortices in smooth shear flows. *Phys. Rev. Lett.* **79**, 3178 – 3181.

Goldstein, M. E.and Afsar, M. Z.and Leib S. J. 2013 Structure of the small amplitude motion on transversely sheared mean flows. *Tech. Rep.* NASA/TM-2013-217862, E-18655. NASA Glenn Research Center; Cleveland, OH, United States.

Hau, J.-N., Chagelishvili, G., Khujadze, G., Oberlack, M. & Tevzadze, A. 2015 A comparative numerical analysis of linear and nonlinear aerodynamic sound generation by vortex disturbances in homentropic constant shear flows. *Phys. Fluids.* **27** (11), 126101.

Hau, J.-N., Oberlack, M. & Chagelishvili, G. 2017 On the optimal systems of subalgebras for the equations of hydrodynamic stability analysis of smooth shear flows and their group-invariant solutions. *J. Math. Phys.* **58** (4), in press.

Lighthill, M. J. 1952 On sound generated aerodynamically – I. General theory. *Proc. Roy. Soc. London Ser. A* **211**, 564–587.

Lighthill, M. J. 1954 On sound generated aerodynamically – II. Turbulence as a source of sound. *Proc. Roy. Soc. London Ser. A* **222**, 1–32.

Lord Kelvin 1887 Stability of fluid motion: Rectilinear motion of viscous fluid between two parallel plates. *Phil. Mag.* **24**, 188–196.

McIntyre, M. E. 2009 Spontaneous imbalance and hybrid vortex–gravity structures. *J. Atmos. Sci.* **66**, 1315–1326.

Moffatt, H. K. 1967 *Interaction of turbulence with strong wind shear*, pp. 139–156. Nauka Press, Moscow.

Schmid, P. J. & Henningson, D. S. 2001 *Stability and transition in shear flows. Applied Mathematical Sciences* Bd. 142. Springer.

Tam, C. K. W. 1995 Supersonic jet noise. *Annu. Rev. Fluid Mech.* **27**, 17–43.

Yoshida, Z. 2005 Kinetic theory for non-hermitian dynamics of waves in shear flow. *Phys. Plasmas* **12**, 024503.